

F irst M easurem ents of the E xclusive D ecays of the $(5S)$ to B
M eson F inal States and Im proved B_s M ass M easurem ent

O .A quines,¹ Z .Li¹ A .Lopez,¹ H .M endez,¹ J .R am irez,¹ G .S .Huang,² D .H .M iller,²
V .Pavlunin,² B .Sanghi,² I .P .J .Shipsey,² B .X in,² G .S .A dam s,³ M .Anderson,³
J .P .C um m ings,³ I .D anko,³ J .N apolitano,³ Q .He,⁴ J .Insler,⁴ H .M uram atsu,⁴ C .S .Park,⁴
E .H .Thomdike,⁴ T .E .Coan,⁵ Y .S .Gao,⁵ F .Liu,⁵ R .Stroynowski,⁵ M .Artuso,⁶
S .Blusk,⁶ J .Butt,⁶ J .Li,⁶ N .M enaa,⁶ R .M ountain,⁶ S .N isar,⁶ K .R andrianarivony,⁶
R .Redjim i,⁶ R .Sia,⁶ T .Skwamicki,⁶ S .Stone,⁶ J .C .W ang,⁶ K .Zhang,⁶ S .E .C soma,⁷
G .Bonvicini,⁸ D .C inabro,⁸ M .Dubrovin,⁸ A .Lincoln,⁸ D .M .A sner,⁹ K .W .Edwards,⁹
R .A .B riere,¹⁰ I .B rock,¹⁰ J .Chen,¹⁰ T .Ferguson,¹⁰ G .Tatishvili,¹⁰ H .V ogel,¹⁰
M .E .W atkins,¹⁰ J .L .Rosner,¹¹ N .E .A dam,¹² J .P .A lexander,¹² K .B erkeman,¹²
D .G .C assel,¹² J .E .D uboscq,¹² K .M .E cklund,¹² R .E hrlich,¹² L .F ields,¹² R .S .G alik,¹²
L .G ibbons,¹² R .G ray,¹² S .W .G ray,¹² D .L .H artill,¹² B .K .H eltsley,¹² D .H ertz,¹²
C .D .Jones,¹² J .K andaswamy,¹² D .L .K reinick,¹² V .E .K uznetsov,¹² H .M ahlke-K ruger,¹²
T .O .M eyer,¹² P .U .E .O nyisi,¹² J .R .P atterson,¹² D .P eterson,¹² E .A .P hillips,¹²
J .P ivarski,¹² D .R iley,¹² A .R yd,¹² A .J .S ado,¹² H .S chwartho,¹² X .S hi,¹²
S .Stroiney,¹² W .M .S un,¹² T .W ilksen,¹² M .W einberger,¹² S .B .A thar,¹³ P .A very,¹³
L .B reva-N ewell,¹³ R .P atel,¹³ V .P otlia,¹³ H .S toedt,¹³ J .Y elton,¹³ P .R ubin,¹⁴
C .C awl eel d,¹⁵ B .I .E isenstein,¹⁵ I .K arliner,¹⁵ D .K im,¹⁵ N .L orey,¹⁵ P .N aik,¹⁵
C .S edlack,¹⁵ M .S elen,¹⁵ E .J .W hite,¹⁵ J .W iss,¹⁵ M .R .S hepherd,¹⁶ D .B esson,¹⁷
T .K .P edlar,¹⁸ D .C ronin-H ennedy,¹⁹ K .Y .G ao,¹⁹ D .T .G ong,¹⁹ J .H ietala,¹⁹
Y .K ubota,¹⁹ T .K lein,¹⁹ B .W .L ang,¹⁹ R .P oling,¹⁹ A .W .S cott,¹⁹ A .S m ith,¹⁹ S .D obbs,²⁰
Z .M etreveli,²⁰ K .K .S eth,²⁰ A .T om aradze,²⁰ P .Z weber,²⁰ J .E rnst,²¹ K .A mm s,²²
H .S everini,²³ S .A .D ytm an,²⁴ W .L ove,²⁴ S .M ehrabyan,²⁴ and V .S avinov²⁴

(CLEO Collaboration)

¹U niversity of Puerto R ico, M ayaguez, Puerto R ico 00681

²P urdue U niversity, W est Lafayette, Indiana 47907

³R ensselaer P olytechnic I nstitute, T roy, N ew Y ork 12180

⁴U niversity of R ochester, R ochester, N ew Y ork 14627

⁵S outhem M ethodist U niversity, D allas, T exas 75275

⁶S yracuse U niversity, S yracuse, N ew Y ork 13244

⁷V anderbilt U niversity, N ashville, T ennessee 37235

⁸W ayne State U niversity, D etroit, M ichigan 48202

⁹C arleton U niversity, O ttawa, O ntario, C anada K 1S 5B 6

¹⁰C amegie M ellen U niversity, P ittsburgh, P ennsylvania 15213

¹¹E nrico F ermi I nstitute, U niversity of C hicago, C hicago, I llinois 60637

¹²C ornell U niversity, I thaca, N ew Y ork 14853

¹³U niversity of F lorida, G ainesville, F lorida 32611

¹⁴G eorge M aison U niversity, F airfax, V irginia 22030

¹⁵U niversity of I llinois, U rband-Cham paign, I llinois 61801

¹⁶I ndiana U niversity, B loomington, I ndiana 47405

¹⁷U niversity of K ansas, L awrence, K ansas 66045

¹⁸Luther College, Decorah, Iowa 52101

¹⁹University of Minnesota, Minneapolis, Minnesota 55455

²⁰Northwestern University, Evanston, Illinois 60208

²¹State University of New York at Albany, Albany, New York 12222

²²Ohio State University, Columbus, Ohio 43210

²³University of Oklahoma, Norman, Oklahoma 73019

²⁴University of Pittsburgh, Pittsburgh, Pennsylvania 15260

Dated: Jan. 25, 2006)

Abstract

Using 420 pb⁻¹ of data collected on the (5S) resonance with the CLEO III detector, we reconstruct B mesons in 25 exclusive decay channels to measure or set upper limits on the decay rate of (5S) into B meson final states. We measure the inclusive B cross-section to be $\langle (5S) \rightarrow B \bar{B} \rangle = (0.176 \pm 0.030 \pm 0.016) \text{ nb}$ and make the first measurements of the production rates of $\langle (5S) \rightarrow B^0 \bar{B}^0 \rangle = (0.131 \pm 0.025 \pm 0.014) \text{ nb}$ and $\langle (5S) \rightarrow B^+ \bar{B}^- \rangle = (0.043 \pm 0.016 \pm 0.006) \text{ nb}$, respectively. We set 90% confidence level limits of $\langle (5S) \rightarrow B^0 \bar{B}^0 \rangle < 0.038 \text{ nb}$, $\langle (5S) \rightarrow B^+ \bar{B}^- \rangle < 0.055 \text{ nb}$ and $\langle (5S) \rightarrow B^+ \bar{B}^0 \rangle < 0.024 \text{ nb}$. We also extract the most precise value of the B_s mass to date, $M(B_s) = (5411.7 \pm 1.6 \pm 0.6) \text{ MeV}/c^2$.

The $(5S)$ resonance was discovered by the CLEO [1] and CUSB [2] collaborations. Its production cross-section and mass were measured to be about 0.35 nb and $(10.865 \pm 0.008)\text{ GeV}/c^2$ [1], respectively. Final states can be: $B\bar{B}$, $B_s\bar{B}_s$, $B_s\bar{B}_s$ and $B_s\bar{B}_s$. Here, $B = B_u$ or B_d , and the \bar{B} may be charged or neutral (consistent with charge zero of the final state). Throughout this article, we use $B\bar{B}$ to signify both $B\bar{B}$ and $B\bar{B}$. Including a symbol in parentheses indicates that it may or may not be present. The $B\bar{B}$ cross-section in this region is well-described by the Unitarized Quark Model (UQM) [3], which predicts that about $1/3$ of the $b\bar{b}$ decay rate is to $B_s^{(\pm)}\bar{B}_s^{(\pm)}$ and that $B\bar{B}$ dominates the inclusive $B\bar{B}$ rate. A previous CLEO measurement using inclusive D_s production revealed that $(5S) \rightarrow B_s^{(\pm)}\bar{B}_s^{(\pm)}$ constitutes $(16.0 \pm 2.6 \pm 5.8)\%$ of the total $b\bar{b}$ rate [4]. A second analysis [5], which performed exclusive reconstruction of B_s mesons found $(e^+e^- \rightarrow B_s\bar{B}_s) = (0.11^{+0.04}_{-0.03} \pm 0.02)\text{ nb}$ (about $1/3$ of the total hadronic resonance cross-section). The two results are consistent with each other and with predictions of the UQM.

In this Letter, we measure the contributions of various B meson final states to the $(5S)$ decay. These measurements may better constrain coupled-channel models in the mass region as well as near the lower resonances [6]. We also exploit exclusively reconstructed B mesons from this analysis and the corresponding B_s analysis [5] to extract the most precise measurement of the B_s mass to date.

CLEO III is a general purpose solenoidal detector that includes a tracking system for measuring momenta and specific ionization (dE/dx) of charged particles, a Ring Imaging Cherenkov detector (RICH) to aid in particle identification, a CsI calorimeter for detection of electromagnetic showers, and a muon system for identifying muons [7].

The analysis presented here uses 420 pb^{-1} of data collected on the $(5S)$ resonance ($\sqrt{s} = 10.868\text{ GeV}$) at the Cornell Electron Storage Ring. Using techniques pioneered at the $(4S)$, we utilize two kinematic variables: the energy difference $E_{\gamma} - E_{\text{beam}} - E_B$ and the beam-constrained mass $M_{bc} = \sqrt{E_{\text{beam}}^2 - p_B^2}$, where E_B (p_B) is the energy (momentum) of the reconstructed B candidate and E_{beam} is the beam energy. Because of its low energy, reconstruction of the photon in $B \rightarrow B\gamma$ is not essential; to maintain high efficiency, we do not reconstruct the $B\gamma$. (Charge conjugate final states are implied throughout this Letter.)

To obtain a B meson sample of higher purity, events are required to have at least five charged tracks and a ratio of the second to zeroth Fox-Wolfram moment [8], $R_2 < 0.25$. Candidate B mesons are reconstructed in exclusive final states containing either J/ψ or $D^{(\ast)}$ mesons.

Charged particles are required to pass standard selection criteria and are identified by using their measured momenta in conjunction with dE/dx , RICH, calorimeter and muon system information. For particle types i, j ($i, j = e, \mu, K, \pi, p$) we define χ^2 -like quantities for dE/dx as the difference in the measured and expected dE/dx , normalized by the uncertainty, i.e., $\chi^2_i = (dE/dx_i^{\text{meas}} - dE/dx_i^{\text{exp}})^2 / \sigma_{dE/dx_i}^2$, and for RICH as $\chi^2_{i;j} = L_i - L_j$ (difference in negative log-likelihood between hypotheses i and j), respectively. We require at least 3 detected Cherenkov photons from the RICH. Pions are identified by requiring $\chi^2_{e\pi} < 4$ or

$\chi^2_{\pi\pi} < 5$. For kaons, we define a combined quantity, $\chi^2_{\text{comb}} = (\chi^2_{eK} / \chi^2_K)^2 + (\chi^2_{\mu K} / \chi^2_K)^2$, and require $\chi^2_{\text{comb}} < 0$. Electron candidates are formed from particles that have a ratio of calorimeter energy (E_e) to measured momentum (p_e) in the range $0.5 < E_e/p_e < 1.25$. Muons are identified by either having penetrated at least 3 layers of iron absorber or by having deposited energy in the calorimeter consistent with a minimum ionizing particle

($E < 300$ MeV). Photons are formed from showers that have deposited at least 30 MeV of energy in the calorimeter and are not associated with a charged track. Pairs of photons that have an invariant mass within 2 standard deviations (≈ 6 MeV/c²) of the known 0 mass (M_0) [9] are defined as 0 candidates and are kinematically constrained to give M_0 .

Candidate $J=$'s are formed from $^+$ or e^+e^- pairs. For muon pairs, we require $3.05 < M_{\mu^+\mu^-} < 3.14$ GeV/c². For e^+e^- combinations with $1.50 < M_{e^+e^-} < 3.14$ GeV/c², bremsstrahlung photons are searched among the showers with no matching charged track and within a 5° cone about each electron's initial direction. For each $^+$ and e^+e^- candidate, we perform a mass-constrained fit to the $J=$ mass [9] and make a loose requirement that the χ^2 per degree of freedom is less than 100. Candidate $^+$ (K_S^0) mesons are formed from $^+^0$ ($^+$) [K^+] combinations that have an invariant mass in the range from 620–920 (490–505) [820–970] MeV/c². D^+ (D^0) meson candidates are reconstructed via their decays to K^+K^+ (K^+, K^+K^- and K^-K^0) and are required to have an invariant mass within 2% of their PDG [9] values. To reduce combinatoric background in $D^0 \rightarrow K^+K^0$, we require $p_T > 400$ MeV/c. Candidate $D^+ \rightarrow D^0\pi^+$ ($D^+ \rightarrow D^0\pi^0$) decays are formed from D^+ and π^0 candidates that have a mass difference in the range $143 < M_{D^+} - M_{D^0} < 147$ MeV/c² ($139 < M_{D^+} - M_{D^0} < 143$ MeV/c²). Similarly, D^0 mesons are reconstructed in $D^0\pi^0$, and the mass difference is required to be in the interval $139 < M_{D^0} - M_{D^0} < 144$ MeV/c².

Candidate B mesons are reconstructed in the 25 decay channels listed in Table I. For $B \rightarrow D^-$ and $B \rightarrow D^-$ [10], we take advantage of the helicity angle (η_h) [11] distribution in these decays and require $|\cos \eta_h| > 0.3$. To improve the signal-to-background ratio, we also reject low momentum (backward-emitted) 0 's from the $^+$ decays by requiring $\cos \eta_h > 0.7$. Table I also shows the product branching fractions, B_i , including the branching ratios of the daughter modes [9], and the reconstruction efficiencies, ϵ_i determined from Monte Carlo simulations [12, 13, 14] of these decays followed by a geant [15] based detector simulation. We validate our simulation and analysis procedure by measuring branching fractions for these decay modes using data collected on the $(4S)$ resonance. Good agreement with the world averages are found for all modes.

We first determine the total B meson yield by fitting the invariant mass distribution formed from candidates in the M_{bc} , E region of $5.272 < M_{bc} < 5.448$ GeV/c², $0.2 < E < 0.45$ GeV. The relatively wide E region is used to avoid biasing the background shape. The invariant mass distribution, shown in Fig. 1, is fit to the sum of a second-order polynomial background and a Gaussian signal shape whose width is fixed to 12.3 MeV/c², the expected average resolution of these candidates. We find a yield of 53.2 ± 9.0 events; fitting to the $J=$ and D^0 distributions individually results in 11.2 ± 3.5 and 42.3 ± 8.4 D^0 events, respectively. Using $B_{\text{total}} = 7.2 \times 10^{-4}$ (see Table I), we measure a cross-section $(4S) \rightarrow B\bar{B}(X) = (0.176 \pm 0.030)$ nb.

Figure 2 shows the reconstructed events in the M_{bc} – E plane for $(4S)$ data. Signal and sideband regions are defined using MC simulations of these final states. To extract rates for $B\bar{B}$, $B\bar{B}$, and $B\bar{B}$ separately, we select events in a signal region defined by the area between the diagonals $M_{bc} = 1.018 E + 5.248$ GeV/c² and $M_{bc} = 1.018 E + 5.312$ GeV/c². This restricted signal region has a total $B_{\text{total}} = 5.7 \times 10^{-4}$. Lower and upper sidebands of the same E width, also shown in Fig. 2, are shifted to the left and right of the signal region by 10 MeV, respectively.

The $B\bar{B}$, $B\bar{B}$, and $B\bar{B}$ final states are kinematically well separated, but $B^0\bar{B}^0$ final

TABLE I: Modes used in exclusive B meson reconstruction along with their product branching fractions (B_i) [9], reconstruction efficiencies (ϵ_i), and expected yields (N_{exp}^i) in data assuming $(5S) \rightarrow B\bar{B}(X) = 0.2 \text{ nb}$.

Mode i	B_i (10^{-4})	ϵ_i (%)	N_{exp}^i
$B^+ \rightarrow J/\psi K^+$	1.18	0.05	43.4 0.9 4.3
$B^0 \rightarrow J/\psi K^0, K^0 \rightarrow K^+$	1.03	0.08	25.6 0.6 2.2
$B^0 \rightarrow J/\psi K_S^0$	0.34	0.02	37.2 1.7 1.1
$B^- \rightarrow D^0, D^0 \rightarrow J/\psi K^+$	1.87	0.09	34.4 0.5 5.4
$B^- \rightarrow D^0, D^0 \rightarrow J/\psi K^+ 0$	6.48	0.56	12.8 0.5 7.0
$B^- \rightarrow D^0, D^0 \rightarrow J/\psi K^+ + 0$	3.67	0.22	20.7 0.7 6.4
$B^- \rightarrow D^0, D^0 \rightarrow J/\psi D^0 0, D^0 \rightarrow J/\psi K^+$	1.08	0.11	11.1 0.5 1.0
$B^- \rightarrow D^0, D^0 \rightarrow J/\psi D^0 0, D^0 \rightarrow J/\psi K^+ 0$	3.76	0.47	2.5 0.2 0.8
$B^- \rightarrow D^0, D^0 \rightarrow J/\psi D^0 0, D^0 \rightarrow J/\psi K^+ + 0$	2.13	0.23	6.9 0.4 1.2
$B^- \rightarrow D^0, D^0 \rightarrow J/\psi K^+ 0$	5.11	0.14	8.2 0.3 3.5
$B^- \rightarrow D^0, D^0 \rightarrow J/\psi K^+ + 0$	17.69	1.36	3.0 0.2 4.5
$B^- \rightarrow D^0, D^0 \rightarrow J/\psi K^+ + + 0$	10.02	0.42	5.2 0.3 4.4
$B^- \rightarrow D^0, D^0 \rightarrow J/\psi D^0 0, D^0 \rightarrow J/\psi K^+$	2.31	0.42	2.1 0.1 0.4
$B^- \rightarrow D^0, D^0 \rightarrow J/\psi D^0 0, D^0 \rightarrow J/\psi K^+ 0$	7.90	1.54	0.7 0.1 0.5
$B^- \rightarrow D^0, D^0 \rightarrow J/\psi D^0 0, D^0 \rightarrow J/\psi K^+ + 0$	4.56	0.84	1.5 0.1 0.6
$B^0 \rightarrow D^+, D^+ \rightarrow J/\psi K^+ + 0$	2.64	0.25	30.9 1.5 6.9
$B^0 \rightarrow D^+, D^+ \rightarrow J/\psi D^0 0, D^0 \rightarrow J/\psi K^+$	0.71	0.06	22.0 0.4 1.3
$B^0 \rightarrow D^+, D^+ \rightarrow J/\psi D^0 0, D^0 \rightarrow J/\psi K^+ 0$	2.47	0.27	4.0 0.1 0.8
$B^0 \rightarrow D^+, D^+ \rightarrow J/\psi D^0 0, D^0 \rightarrow J/\psi K^+ + 0$	1.40	0.12	12.2 0.4 1.4
$B^0 \rightarrow D^+, D^+ \rightarrow J/\psi D^+ 0, D^+ \rightarrow J/\psi K^+ + 0$	0.78	0.08	7.3 0.5 0.5
$B^0 \rightarrow D^+, D^+ \rightarrow J/\psi K^+ + + 0$	7.08	1.28	6.6 0.4 3.9
$B^0 \rightarrow D^+, D^+ \rightarrow J/\psi D^0 0, D^0 \rightarrow J/\psi K^+$	1.75	0.24	4.3 0.2 0.6
$B^0 \rightarrow D^+, D^+ \rightarrow J/\psi D^0 0, D^0 \rightarrow J/\psi K^+ 0$	6.08	0.93	1.3 0.1 0.7
$B^0 \rightarrow D^+, D^+ \rightarrow J/\psi D^0 0, D^0 \rightarrow J/\psi K^+ + 0$	3.44	0.48	2.7 0.2 0.8
$B^0 \rightarrow D^+, D^+ \rightarrow J/\psi D^+ 0, D^+ \rightarrow J/\psi K^+ + 0$	1.94	0.29	1.7 0.1 0.3
Total	$\sum B_i = 72$	10^4	60.4

states have a large degree of overlap, and with the limited statistics cannot be distinguished. The $B\bar{B}$ final states, because of the limited phase space, peak at $M_{bc} \approx E_{\text{beam}}$. If their rate is large enough, their shape (in M_{bc}) will be sufficient to distinguish them from the broad tail of $B^0 \rightarrow D^0 \rightarrow D^+ \bar{D}^-$ final states that extend into the M_{bc} region of $B\bar{B}$.

Events in the signal region of Fig. 2 are projected onto the M_{bc} axis (see Fig. 3) and fit to the sum of a flat background and three Gaussian signals, one each for $B\bar{B}$, $B\bar{B}$ and $B\bar{B}$. The signal resolutions are set to $\sigma = 4.0, 6.2$ and $7.0 \text{ MeV}/c^2$, respectively, as determined from MC simulation, and the background is fixed to 0.7 events/4 MeV, as determined from the average of the upper and lower sidebands. In the fit we use the precisely known mass difference $M_{B^0} - M_{B^-}$ [9] and constrain its value to $47.5 \text{ MeV}/c^2$ [16]. The middle $B\bar{B}$ peak

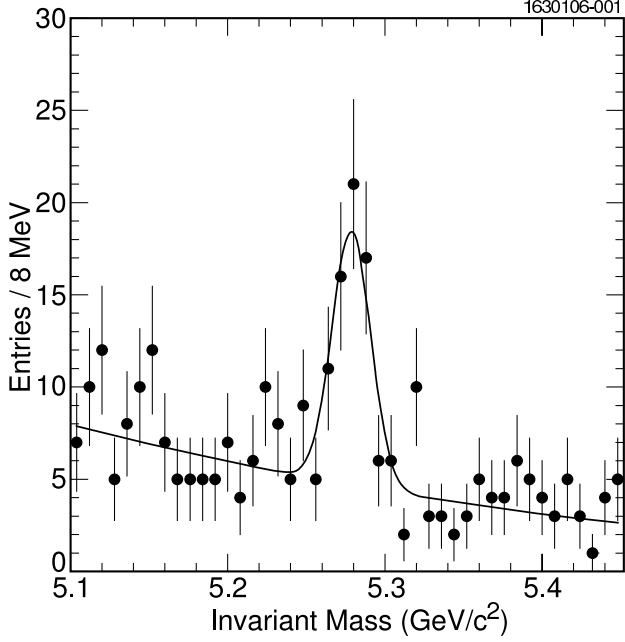


FIG. 1: The B meson invariant mass distribution for all B decay modes listed in Table I in $(5S)$ data. The points are the data and the curve is the t described in the text.

is not constrained in the t , and is found to be within 1% of the expected value.

The fitted yields are $3.7^{+3.1}_{-2.4}$ $B\bar{B}$, $10.3^{+3.9}_{-3.9}$ $B\bar{B}$ and $31.4^{+6.1}_{-6.1}$ $B\bar{B}$ events. Only the latter two are statistically significant with significances, determined from the change in log-likelihood when the contribution from each peak is removed, of 4.3 and 7.6, respectively. For $B\bar{B}$, we compute an upper limit of 7.5 events at 90% confidence level (CL). A potential excess in $B^{(\prime)}\bar{B}^{(\prime)}$ is examined by plotting the invariant mass of candidates in the $B^{(\prime)}\bar{B}^{(\prime)}$ region defined by $5.351 < M_{bc} < 5.429 \text{ GeV}/c^2$ and $0.2 < E < 0.45 \text{ GeV}$, which should exhibit a peak at M_B (see inset in Fig. 3). This M_{bc} – E region includes (88–6)% of reconstructed $B^{(\prime)}\bar{B}^{(\prime)}$ events, where the uncertainty reflects the maximum variation based on the possible $B^{(\prime)}\bar{B}^{(\prime)}$ final states. That distribution is fit to the sum of a Gaussian signal whose mean and rms width are constrained to $5.279 \text{ GeV}/c^2$ and $12.3 \text{ MeV}/c^2$, respectively, and a linear background shape. The yield of $6.7^{+5.1}_{-4.5}$ is not statistically significant, and we compute an upper limit of 13.1 events at 90% CL.

For the $B\bar{B}$ final state, we select events in the region $5.429 < M_{bc} < E_{beam} \text{ GeV}/c^2$ and $0.2 < E < 0.45 \text{ GeV}$ and find three events consistent with M_B . This additional requirement on M_{bc} and E has an efficiency of (95–2)%. While the combinatorial background is small (~0.3 events), the cross-feed from $B^{(\prime)}\bar{B}^{(\prime)}$ into the $B\bar{B}$ signal region is (12–6)%, and given the measured upper limit on $(5S) \rightarrow B^{(\prime)}\bar{B}^{(\prime)}$, we cannot discount that the three events are $B^{(\prime)}\bar{B}^{(\prime)}$. We therefore set an upper limit on $(5S) \rightarrow B\bar{B}$ of 6.4 [17] events at 90% CL. For illustration, we superimpose on Fig. 3, $6.7 B^{(\prime)}\bar{B}^{(\prime)}$ (lightly shaded, with a ratio of 1:1 ratio for $B\bar{B}$ – $B\bar{B}$ – $B\bar{B}$) and 3 $B\bar{B}$ (darker shading) events. Yields, efficiencies, cross-sections and relative production fractions are summarized in Table II. We also show the cross-sections as determined from the $J=1$ and $D^{(\prime)}$ modes separately. We find that $B\bar{B}$ is indeed dominant, comprising (74–15)% of the $B\bar{B}$ (X).

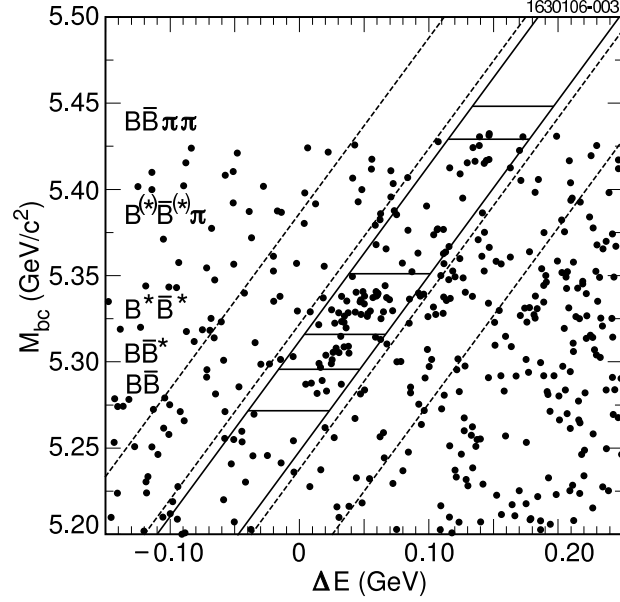


FIG. 2: Scatter plots of M_{bc} vs. ΔE for all B decay modes listed in Table I in (5S) data. The diagonal lines show the expected signal (solid) and 2 sideband (dashed) regions, as discussed in the text. The horizontal lines show the regions for the various $B\bar{B}$ (χ) final states.

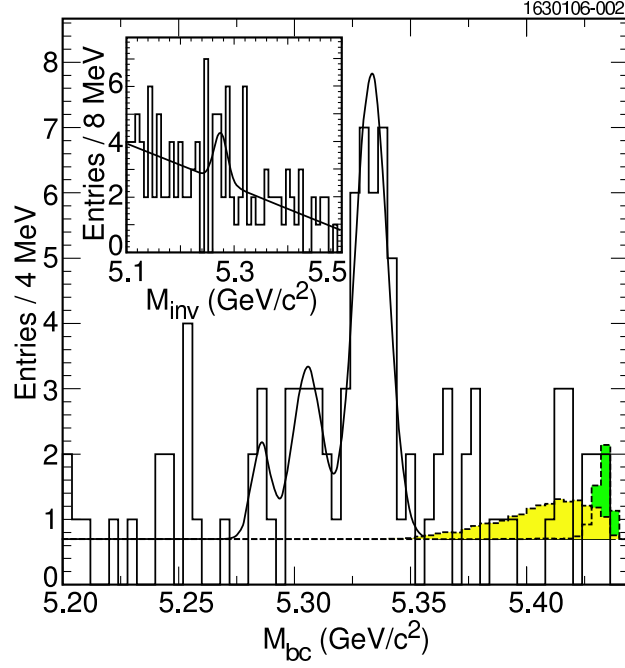


FIG. 3: Distribution of M_{bc} for all reconstructed B modes listed in Table I for (5S) data. The histogram displays the data, the curve shows the fit described in the text and the flat line shows the background as determined from a fit to the sidebands as discussed in the text. Distributions for $B^{(*)}B^{(*)}$ (lightly shaded) and $B\bar{B}$ (darker shading) obtained from MC simulation of these final states are superimposed for illustrative purposes. The inset shows the invariant mass of candidates in the $B^{(*)}B^{(*)}$ M_{bc} region with the fit superimposed.

rate.

Several sources of systematic uncertainty on the cross-sections measurements are considered. Potential errors from the background normalization and shape are evaluated by using different background parameterizations and varying the normalization within its uncertainty. The corresponding uncertainties in the cross-sections vary from 3.1% for $(5S) \rightarrow B\bar{B}(X)$ to 16.7% for $B\bar{B}$. Reconstruction efficiencies from the simulation for all modes are cross-checked by measuring B branching fractions using data collected on the $(4S)$ resonance and comparing their values to the world averages [9]. Averaged over all modes, we find an agreement of (1–3)%, and we conservatively assign a 5% systematic uncertainty to the efficiencies determined from simulation. When combined with the limited MC statistics, we find an overall uncertainty in the reconstruction efficiency of 6.4%. Errors due to the fixed signal shape parameters are determined by varying them within their uncertainties and re-titting (3%–4%). The occurrence of multiple candidates in data (in a single event) are found to agree with simulation to within 3%. Uncertainties on input branching fractions and measured integrated luminosity contribute 3% and 2%, respectively. These systematic uncertainties are added in quadrature and the resulting values are included in the cross-sections shown in Table II.

TABLE II: Summary of yields, efficiencies, cross-sections and fractional contributions of various subprocesses in $(5S) \rightarrow B\bar{B}(X)$ decays. Upper limits are set at the 90% CL. Uncertainties are from statistical and systematic sources, respectively.

$(5S) \rightarrow B\bar{B}(X)$	Yield (# Events)	Efficiency (10^{-4})	Cross-Section (nb)	$\mathcal{M} = (5S) \rightarrow B\bar{B}(X)$ (%)						
$B\bar{B}$	< 7.5	5.7	0.4	< 0.038						
$B\bar{B}$	10.3	3.9	5.7	0.4	0.043	0.016	0.006	24	9	3
$B\bar{B}$	31.4	6.1	5.7	0.4	0.131	0.025	0.014	74	15	8
$B\bar{B}^{\prime\prime}$	< 13.1	6.3	0.6		< 0.055			< 32		
$B\bar{B}$	< 6.4	6.8	0.5		< 0.024			< 14		
$(5S) \rightarrow B\bar{B}(X)$	53.2	9.1	7.2	0.5	0.176	0.030	0.016			
$\mathcal{M} = \text{M modes}$	11.2	3.5	6.3	0.5	0.295	0.092	0.028			
$D^{\prime\prime} \rightarrow M \bar{M}$ modes	42.3	8.4	0.9	0.1	0.160	0.032	0.015			

We proceed to use the M_{bc} distribution from this analysis in combination with the one for B_s in Ref. [5] to obtain an improved measurement of the B_s mass. Since those results used exactly the same data set as in this analysis, the largest systematic error, the beam energy calibration of ($+4.6 \pm 2.9$) MeV [5], cancels out in the (uncorrected) M_{bc} difference, $M_{bc}(B_s) - M_{bc}(B)$. Using the M_{bc} peak positions of (5333.1 ± 1.3) MeV/ c^2 (this analysis) and $(5418.1 \pm 1.0 \pm 3.0)$ MeV [18] for B and B_s , respectively, we find a mass difference $M(B_s) - M(B) = (86.7 \pm 1.6 \pm 0.2)$ MeV/ c^2 . Here, M_{bc} has been replaced by mass M after incorporating a -1.7 ± 0.1 MeV/ c^2 shift reflecting a bias that is introduced due to our use of reconstructed $B_{(s)}$ instead of $B_{(s)}$ mesons. The 1.6 MeV/ c^2 error is statistical and the 0.2 MeV/ c^2 uncertainty is from systematic errors in fitting our M_{bc} spectrum. Combining this mass difference with $M(B) = (5325.0 \pm 0.6)$ MeV/ c^2 [9], we obtain an improved value for the B_s mass, $M(B_s) = (5411.7 \pm 1.6 \pm 0.6)$ MeV/ c^2 . Using the well-measured B_s mass

from CDF of $M(B_s) = (5366.01 \pm 0.73 \pm 0.33) \text{ MeV}/c^2$ [19], we determine the $1^0 0^-$ mass splitting $M(B_s) - M(B_s^0) = (45.7 \pm 1.7 \pm 0.7) \text{ MeV}/c^2$. This mass splitting measurement supersedes the previous CLEO result [5] of $(48 \pm 1 \pm 3) \text{ MeV}/c^2$ [5] and is significantly more precise than an earlier indirect measurement of $(47.0 \pm 2.6) \text{ MeV}/c^2$ [20]. It is also consistent with the corresponding splitting in the B_d system of $(45.78 \pm 0.35) \text{ MeV}/c^2$ [9] as expected from heavy-quark symmetry [21].

In summary, we have measured or set upper limits on the rates for the various final states in $(5S)$ decay. We find that predictions of the UQM [3] are consistent with our findings that $B \bar{B}$ is dominant, with a measured value of $(74 \pm 15)\%$ of the total B rate. The $B \bar{B}$ rate is measured to be about $1/3$ of the $B \bar{B}$ rate. Upper limits on $B \bar{B}$, $B^{(0)} \bar{B}^{(0)}$ and $B \bar{B}^0$ have also been presented. Lastly, we utilized the M_{bc} peak positions for B_s and B_s^0 [5] to extract $M(B_s) = (5411.7 \pm 1.6 \pm 0.6) \text{ MeV}/c^2$, which is the most precise value of the B_s mass to date.

We gratefully acknowledge the effort of the CESR staff in providing us with excellent luminosity and running conditions. This work was supported by the Alfred P. Sloan Foundation, the National Science Foundation, and the U.S. Department of Energy.

- [1] D. Besson et al. (CLEO Collaboration), *Phys. Rev. Lett.* **54**, 381 (1985).
- [2] D. M. Lovelock et al. (CUSB Collaboration), *Phys. Rev. Lett.* **54**, 377 (1985).
- [3] N. Tornqvist, *Phys. Rev. Lett.* **53**, 878 (1984); S. Ono, N. Tornqvist, J. Lee-Franzini and A. Sanda, *Phys. Rev. Lett.* **55**, 2938 (1985); S. Ono, A. Sanda and N. Tornqvist, *Phys. Rev. D* **34**, 186 (1986).
- [4] M. Artuso et al. (CLEO Collaboration), *Phys. Rev. Lett.* **95**, 261801 (2005) [[hep-ex/0508047](#)].
- [5] G. Bonvicini et al. (CLEO Collaboration), *Phys. Rev. Lett.* **96**, 022002 (2006) [[hep-ex/0510034](#)].
- [6] E. Eichten et al., *Phys. Rev. D* **21**, 203 (1980).
- [7] D. Peterson et al., *Nucl. Instrum. Meth. A* **478**, 142 (2002); M. Artuso et al., *Nucl. Instrum. Meth. A* **554**, 147 (2005); Y. Kubota et al., *Nucl. Instrum. Meth. A* **320**, 66 (1992).
- [8] G. C. Fox and S. W. Golfram, *Phys. Rev. Lett.* **41**, 1581 (1978).
- [9] S. Eidelman et al., *Phys. Lett. B* **592**, 1 (2004) and 2005 partial update for the 2006 edition available on the PDG WWW pages (<http://pdg.lbl.gov/>).
- [10] S. E. Czoma et al. (CLEO Collaboration), *Phys. Rev. D* **67**, 112002 (2003).
- [11] For this decay, the helicity angle η is the angle between the 0^0 direction in the rest frame and the direction in the D^0 rest frame.
- [12] T. Sjstrand et. al., *Computer Phys. Commun.* **135**, 238 (2001) [LU TP 00-30, [hep-ph/0010017](#)].
- [13] QQ - The CLEO Event Generator, <http://www.lns.cornell.edu/public/CLEO/soft/QQ>.
- [14] E. Barberio and Z. W. Was, *Comput. Phys. Commun.* **79**, 291 (1994).
- [15] R. Brun et al., GEANT 3.21, CERN Program Library Long Writeup W 5013 (unpublished), 1993.
- [16] The $B \rightarrow B_s$ mass difference is $45.78 \pm 0.35 \text{ MeV}/c^2$, to which a $1.7 \text{ MeV}/c^2$ Lorentz boost correction was applied that reflects our use of the B_s meson momentum in computing M_{bc} rather than the B momentum.
- [17] G. Feldman and R. Cousins, *Phys. Rev. D* **57**, 3873 (1998).

- [18] This value is reduced by the beam energy correction of 4.6 MeV which was applied in Ref. [5].
- [19] D. A. Costa et al. (CDF Collaboration), submitted to Phys. Rev. Lett. [hep-ex/0508022].
- [20] J. Lee-Franzini et al. (CUSB Collaboration), Phys. Rev. Lett. 65, 2947 (1990).
- [21] W. Bardeen, E. Eichten and C. Hill, Phys. Rev. D 68, 054024 (2003), and references therein.